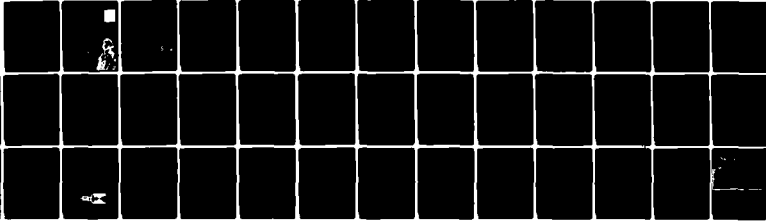
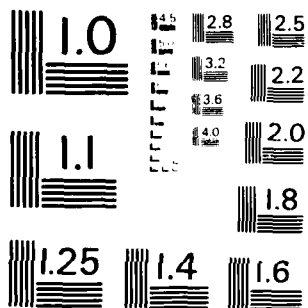


AD-A145 824 FATIGUE CRACK PROPAGATION IN METASTABLE TITANIUM ALLOYS 1/1  
(U) GEORGE WASHINGTON UNIV WASHINGTON DC SCHOOL OF  
ENGINEERING AN... S H YANG ET AL. JUL 84  
UNCLASSIFIED GWU-CMEE-TR-84-1 N00019-82-C-0170 F/G 20/11 NL



END  
DATE  
FILMED  
10-84  
DTIC



MICROCOPY RESOLUTION TEST CHART  
NATIONAL BUREAU OF STANDARDS - 1963 - A

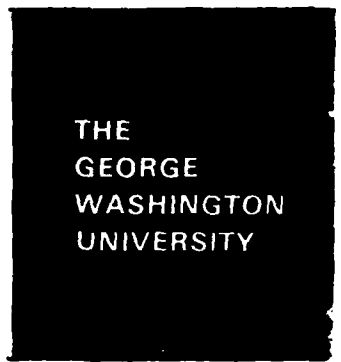
AD-A145 824

t

Fatigue Crack Propagation in  
Metastable Titanium Alloys

by

S. H. Yang, A. Raith, C. M. Gilmore  
and M. A. Imam



THE  
GEORGE  
WASHINGTON  
UNIVERSITY

STUDENTS FACULTY STUDY  
RESEARCH DEVELOPMENT FUTURE CAREER CREATIVITY COMMUNITY LEADERSHIP TECHNOLOGY FRONTIERS DESIGN ENGINEERING APPLICATIONS GEORGE WASHINGTON UNIVERSITY



DTIC FILE COPY

SEP 21 1984

APPROVED FOR PUBLIC RELEASE  
DISTRIBUTION UNLIMITED

SCHOOL OF ENGINEERING  
AND APPLIED SCIENCE

1 10 48



TABLE OF CONTENTS

	<u>Page No.</u>
Abstract.....	1
Introduction.....	1
Experimental Procedure.....	2
Results.....	6
Discussion.....	7
Conclusions.....	9
References.....	10
List of Tables .....	12
List of Figures.....	13

#### ABSTRACT

The fatigue crack growth rate tests of water quenched Corona-5 (Ti-4.5Al-1.5Cr-5Mo) and Ti-6Al-4V alloy were conducted in air at room temperature. The effect of the presence of the metastable retained  $\beta$  phase on the fatigue crack growth rate was examined in this research. The specimens were heat treated and water quenched to have unstable  $\beta$  phase that could be transformed to martensite during the fatigue crack growth testing. As quenched specimens were compared with specimens in the mill annealed condition. The fatigue crack growth rates of all the specimens were in the same order of magnitude regardless of the heat treatment. From this research it was shown that in Corona-5 and Ti-6Al-4V alloys the fatigue crack growth rates were not affected by the strain induced martensitic transformation. The yield strength of the specimens in this research varied from 337 Mpa [48.9 ksi] to 947 Mpa [137 ksi]. This also demonstrated that the fatigue crack growth rates of Corona-5 and Ti-6Al-4V alloys in these conditions were independent of the yield strength.

## INTRODUCTION

The alloys Corona-5 (Ti-4.5Al-1.5Cr-5Mo) and Ti-6Al-4V were both developed as  $\alpha+\beta$  alloys where Cr, Mo and V are the  $\beta$  (B.C.C) stabilizers (which decrease the  $\beta$  transus temperature) and Al is an  $\alpha$  (H. C. P) stabilizer (which raises the  $\beta$  transus temperature). It was observed by several investigators [1,2,3] that in the  $\alpha+\beta$  microstructure the Corona-5 alloy had high strength, high fracture toughness and excellent corrosion resistance, but it was also observed that Corona-5 had high fatigue crack growth rates ( $da/dN$ ) at low stress intensity range ( $\Delta k$ ) [1]. Imam and Gilmore [4,5] observed that the metastable  $\beta$  phase was retained when the Ti-6Al-4V alloy was water quenched from just below the  $\beta$  transus temperature. The transformation of the metastable  $\beta$  to  $\alpha'$  by mechanical strain through a strain induced martensitic transformation was observed to improve the low cycle fatigue lives of both the alloys Corona-5 and Ti-6Al-4V [4,5,6].

In Fe-16Cr-13Ni stainless steel, Pineau and Pelloux [7] investigated the influence of the strain induced martensitic transformation on the fatigue crack growth rate. They reported that for a given stress intensity range ( $\Delta k$ ) the fatigue crack growth rate ( $da/dN$ ) in stainless steel was decreased as the volume of the strain induced martensite increased at the crack tip. The purpose of this research was to examine the effect of the presence of metastable  $\beta$  phase and its strain induced transformation to martensite on the fatigue crack growth rate in the alloys Corona-5 and Ti-6Al-4V. For this purpose, the fatigue crack growth rates of quenched Corona-5 with metastable  $\beta$  and without metastable  $\beta$  and mill annealed Corona-5 were compared. The fatigue crack growth rates of quenched Ti-6Al-4V with metastable  $\beta$  and  $\alpha+\beta$  annealed Ti-6Al-4V were also compared.

## EXPERIMENTAL PROCEDURE

### Materials

Two different alloys, Corona-5 (Ti-4.5Al-1.5Cr-5Mo) and Ti-6Al-4V were used in this experiment. The Corona-5 plate was obtained from Colt Industries (plate E from heat R 52071) [1]. The mill anneal condition of this alloy was low  $\beta$  processed and the  $\beta$  transus temperature was reported to be 938°C. (1720°F). The heat chemistry in weight percentage was reported to be:

Al	Mo	Cr	O	N	Fe	H	C	Ti
4.4	5.1	1.46	0.183	0.011	0.20	0.0018	0.65	balance

The alloy Ti-6Al-4V was provided by the Naval Ship Research and Development Lab, Annapolis, MD (Heat No. 29555-06) as 3.75 cm (1.25 in) thickness plate and the heat chemistry in weight percentage was reported to be:

Al	V	Fe	O	N	C	H
6.0	3.9	0.18	0.117	0.010	0.02	0.020.

This alloy was  $\beta$  processed at 1066°C and mill annealed at 1024°C for 5 minutes and air cooled.

### Heat Treatment

Heat treatments were performed to produce varying amounts of the metastable retained  $\beta$  phase. The Corona-5 alloy was water quenched after 30 minutes heat treatment at 965°C (37°C above the  $\beta$  transus) to produce a fully martensitic microstructure, and other specimens were water quenched from 915°C, 900°C and 870°C (below the  $\beta$  transus) to produce increasing amounts of retained  $\beta$  phase.

It was observed by Gilmore et.al., [6] that Corona-5 water quenched from 915°C had the longest fatigue life of any of the mill annealed or water quenched conditions studied. Specimens of Corona-5 were also prepared in the mill annealed condition to serve as a reference. Ti-6Al-4V alloy water quenched from 900°C was shown to have the highest fatigue life of any water quenched conditions studied and this heat treatment was chosen for the fatigue crack growth rate tests [4]. The Ti-6Al-4V alloy was water quenched after heat treatment at 900°C for 1 hour. Specimens of Ti-6Al-4V were also prepared in the  $\alpha+\beta$  annealed condition: 800°C for 3 hours then a furnace cool to 600°C followed by air cooling to room temperature. The  $\alpha+\beta$  anneal in Ti-6Al-4V alloy served as a reference for comparison with the as quenched condition.

#### Fatigue Crack Growth Rate Tests

The fatigue crack growth rate tests were performed in air at room temperature. Tests were conducted in accordance with ASTM E-647, the standard test method for constant-load-amplitude fatigue crack growth rates above  $10^{-8}$ m/cycle. A MTS 810 series electrohydraulic closed loop Material Testing System was used for these tests. The specimens for these tests were of the wedge opening loaded (WOL) type as presented in Figure 1. A clip gage was used to obtain crack opening displacement. The clip gage was fixed to the specimen at the crack mouth via knife edges mounted on the specimen as shown in Figure 2. The sensitivity of the clip gage was 10.06 mv per  $10^{-2}$  cm crack opening displacement.

At the beginning of the crack propagation test with a known machined notch size, the Young's modulus was obtained from the equation [8]:

$$E = \frac{P}{B[\text{COD}]} * f(a/w) \quad (1)$$

$$f(a/w) = \left( 1 + \frac{0.2549}{a/w} \right) \left( \frac{1+a/w}{1-a/w} \right)^2 [4.3838 - 37.588(a/w) + 359.68(a/w)^2 - 1319.5(a/w)^3 + 2506.8(a/w)^4 - 2577.0(a/w)^5 + 1203.5(a/w)^6 - 136.4(a/w)^8]$$

where P is applied load, B the thickness of the specimen, COD the crack opening displacement, "a" the crack length and w the wedge length.

The maximum stress intensity factor  $K_{\max}$  was controlled to within 5 percent during the precracking in accordance with ASTM E-647. After the fatigue precrack was initiated, the load was reduced no more than 20 percent per step to the desired level for crack propagation tests.

Fatigue crack growth rate tests were performed with tension-tension haversine cyclical loading of frequency 10 Hz. with a load ratio of R=0.1. The load versus crack opening displacement was nonlinear at low load as shown in Figure 3. Therefore the COD from the clip gage was determined from the following expression [10]:

$$\text{COD} = 2 * (\text{COD}_{\max} - \text{COD}_{1/2\max}) \quad (2)$$

$\text{COD}_{\max}$  and  $\text{COD}_{1/2\max}$  were measured by statically loading to  $P_{\max}$  and  $P_{1/2\max}$  respectively.

Crack length was calculated from the COD measurement using the following expression [8]:

$$a/w = C_0 + C_1(U_x) + C_2(U_x)^2 + C_3(U_x)^3 + C_4(U_x)^4 + C_5(U_x)^5 \quad (3)$$

where

$$U_x = \frac{1}{\left( \frac{BE[COD]}{P} \right)^{1/2} + 1}$$

$$\begin{aligned} C_0 &= 1.0021, & C_1 &= -4.9472, & C_2 &= 35.749 \\ C_3 &= -649.85, & C_4 &= 4110.9, & C_5 &= -8410.8 \end{aligned}$$

The crack growth rate (da/dN) was obtained using the incremental seven point polynomial method which is recommended in ASTM E-647. The crack length ( $a_i$ ) obtained from incremental method is given by :

$$a_i = b_0 + b_1 \left( \frac{N_i - C_1}{C_2} \right) + b_2 \left( \frac{N_i - C_1}{C_2} \right)^2 \quad (4)$$

where

$$C_1 = 0.5(N_{i-n} + N_{i+n})$$

$$C_2 = 0.5(N_{i+n} - N_{i-n})$$

$b_0$ ,  $b_1$ , and  $b_2$  are regression parameters which are determined by the least square criterion over the local range of crack growth.

The rate of crack growth at  $N_i$  was obtained from the derivatives of the above parabolic equation:

$$\left. \frac{da}{dN} \right|_{a_i} = \frac{b_1}{C_2} + \frac{2b_2(N_i - C_1)}{C_2^2} \quad (5)$$

Stress intensity range ( $\Delta K$ ) was obtained using the following expression [8]:

$$\Delta K = \frac{\Delta P}{B\sqrt{w}} \frac{(2+a/w)}{(1-a/w)^{3/2}} * [0.8072 + 8.858 (a/w) - 30.23(a/w)^2 + 41.088(a/w)^3 - 24.15(a/w)^4 + 4.951(a/w)^5] \quad (6)$$

All of the above data were analyzed and plotted on a log-log scale utilizing the fatigue crack growth rate test software for the data collection, analysis and plotting, developed at the George Washington University which enhanced the accuracy of the test results.

#### RESULTS

The results of the fatigue crack growth rate tests that are presented in Tables 1 to 7 and graphically presented in Figures 4 to 10 indicated that the fatigue crack propagation rate in each specimen was independent of heat treatment. All the data for Corona-5 is plotted in Figure 11 and it clearly shows that fatigue crack growth rate was not significantly affected by the strain induced martensitic transformation. In the alloy Corona-5 quenched from 965°C and Ti-6Al-4V quenched from 900°C, the crack path deviated by more than 5 degrees from the horizontal plane for  $\Delta K$  values above 12 Mpa and 16 Mpa respectively. Therefore, the results were invalid above these  $\Delta K$  values as indicated in Figure 7 and 9. The fatigue crack growth rate of Corona-5 water quenched from 915°C was very low at the stress intensity range ( $\Delta K$ ) between 14 and 16 MPa. The crack growth rate at low  $\Delta K$  (8.4 Mpa) in the mill annealed Corona-5 was higher than any other treatments. The fatigue crack growth rates of as quenched and  $\alpha+\beta$ annealed Ti-6Al-4V alloys were same order of magnitude and indicated independency of the heat treatment.

## DISCUSSION

The most interesting result from this research was the observation that the fatigue crack propagation was independent of the heat treatment. This was unexpected because previous work on steels [7] had shown that fatigue crack propagation rate was strongly affected when a strain induced martensitic transformation was present. In addition, the heat treatments utilized in this research resulted in a large (nearly 300 percent) change in yield strength as shown in Tables 8 and 9. From the research of Crooker [11], a decrease in crack propagation rate would be expected with a decrease in yield strength. The results of this research possibly provide some insight into the important parameters that effect the fatigue crack propagation rate.

In this research on titanium alloys the presence of the strain induced martensitic transformation had no effect on the fatigue crack propagation rate; however, there was a significant effect in stainless steel as observed by Pineau and Pelloux [7] and in TRIP steel as observed by Chanani [12]. Pineau and Pelloux discussed several possible mechanisms that could have resulted in the reduced crack propagation rates that they observed in metastable alloys. One mechanism was the rapid strain hardening that was observed in the steels and is also present in the metastable titanium alloys. Pineau and Pelloux concluded that the strain hardening mechanism was not sufficient to explain the magnitude of the observed changes in crack propagation rate. The result reported here would support that conclusion because in the very low yield strength titanium alloys there was rapid strain hardening and in the high strength titanium alloys there was essentially no strain hardening, and yet there was no effect on the fatigue crack propagation rate.

Thus on the basis of our results strain hardening would appear to not be a dominating factor of the fatigue crack propagation rate in these titanium alloys. Crooker [11] has proposed that fatigue crack propagation rates increased linearly with increases in yield strength. Also, on the basis of theories that relate fatigue crack propagation rates to  $K_{Ic}$  values, a high yield strength and low strain hardening rate should result in a higher crack propagation rate according to the equations of Forman [13] and Hirth [14]. However, this result was not obtained in this research. It has been proposed by a number of authors [15,16] that the ultimate tensile strength is a dominating factor determining  $K_{Ic}$  and the resulting fatigue crack propagation rate. In this research the ultimate tensile strength was relatively constant, and in all of the heat treatments the crack propagation rate was relatively constant. This research would support the relationship between ultimate tensile strength and fatigue crack propagation rate.

One significant difference in the martensitic transformation in the steels and titanium alloys is that in the steels a large volume increase (typically 5 to 8 percent) occurs as a result of the martensitic transformation. However, based upon the lattice parameters of Imam and Gilmore [4], a volume decrease of 1.1 percent was calculated for Ti-6Al-4V quenched from 900°C when transforming from BCC to HCP. A volume increase as a result of the strain induced martensitic transformation would produce compressive residual stresses at the crack tip that would reduce the crack propagation rate and a volume decrease should produce tensile residual stress.

Since this difference in volume change was one of the major differences between the martensitic transformation in titanium alloys and the steels, it appears that the volume change that occurred during the martensitic transformation was a major factor in the decrease in crack propagation rates observed in the steels.

#### CONCLUSIONS

From the fatigue crack growth rate tests of Corona-5 and Ti-6Al-4V, it was concluded that:

1. The fatigue crack growth rates of Corona-5 and Ti-6Al-4V alloys were not significantly affected by the presence of a metastable  $\beta$  phase and its strain induced transformation to martensite.
2. The fatigue crack growth rate of Corona-5 was independent of yield strength in the conditions tested.
3. The change in volume during the strain induced martensitic transformation at the crack tip appears to have a significant effect on the fatigue crack propagation rates. Large increases in volume would result in large compressive residual stresses at the crack tip reducing the crack propagation rates.

#### REFERENCES

1. G. R. Keller, J. C. Chesnutt, F.H. Froes and C.G. Rhodes, "Fracture Toughness in Titanium Alloy", Final Engineering Report, Naval Air Systems Command Contract N00019-76-C-0427 NA-78-917 (1978)
2. F. H. Froes and W. T. Highberger, J. Metals, **32**, (1980) 57-64.
3. G. R. Keller, J. C. Chesnutt, W. T. Highberger, C. G. Rhodes and F. H. Froes, "The Relationship of Processing/ Microstructure/Mechanical Properties for the Alpha-Beta Titanium Alloy Ti-4.5Al-1.5Cr-5Mo (Corona-5)", in Titanium'80 **2**, (ed. H. Kumura and O. Izumi), The Metallurgical Society of AIME, Warrendale, Pennsylvania , 1980, p. 1210-1220.
4. M.A. Imam and C. M. Gilmore, Met Trans A., **14A**, (1983),233.
5. M. A. Imam and C. M. Gilmore, "New Observations of the Transformation in Ti-6Al-4V", in Titanium 80, **2**, (ed. H. Kimura and O. Izumi), The Metallurgical Society of AIME, Warrendale, Pennsylvania, 1980, p. 1533-42.
6. C. M. Gilmore, S. Yang, M.A. Imam, A. Fraker and A. Van Orden, "The Mechanical and Microstructural Properties of Quenched and Aged Ti-4.5Al-5Mo-1.5Cr", Final Engineering Report, Naval Air Systems Command Contract N00019-80-C-0403 (1983)
7. A. G. Pineau and R. M. Pelloux, MET Trans., **5**, (1974) 1103.
8. A. Saxena and S. J. Hudak, Jr., Intl. J. of Fracture, **14**, (1978) 453-468.
9. ASTM E 647-81, "Standard Test Method for Constant-load Amplitude Fatigue Crack Growth Rates above  $10^{-8}$ m/cycle", 1981 Annual Book of ASTM Standards, **10**, American Society for Testing and Materials, Philadelphia, Pennsylvania, 1981, p. 765-785.
10. G. R. Yoder, L. A. Cooley and T. W. Crooker, "Procedure for Precision Measurement of Fatigue Crack Growth Rate Using Crack Opening Displacement Techniques", ASTM STP, **738** (1981).
11. T. W. Crooker and D. J. Krause, "Fatigue Crack Growth Rates in Ti-6Al-4V Alloy at Various Yield Strength and Fracture Toughness Levels", Report of NRL Progress (NRL Problem No.: M01-25), (1972).
12. G. R. Chanani, S. D. Antolovich and W. W. Geberich, Met. Trans., **3**, (1972) 166-167.
13. R. G. Forman, V. E. Kearney and R. M. Engle, J. of Basic Engineering, (1967), 459-464.

REFERENCES  
(continued)

14. J. P. Hirth and F. H. Froes, Met. Trans., 8A, (1977) 1167-1176.
15. J. M. Krafft, Appl. Mech. Research, 3, (1963) 88.
16. R.G. Hoagland, A. R. Rosenfield, and G. T. Hahn, Met. Trans., 3A, (1972) 123.

LIST OF TABLES

- Table 1. Fatigue Crack Propagation Data of Corona-5 Quenched from 870°C
- Table 2. Fatigue Crack Propagation Data of Corona-5 Quenched from 900°C
- Table 3. Fatigue Crack Propagation Data of Corona-5 Quenched from 915°C
- Table 4. Fatigue Crack Propagation Data of Corona-5 Quenched from 965°C
- Table 5. Fatigue Crack Propagation Data of Mill Annealed Corona-5
- Table 6. Fatigue Crack Propagation Data of  $\alpha+\beta$  Annealed Ti-6Al-4V
- Table 7. Fatigue Crack Propagation Data of Ti-6Al-4V Quenched from 900°C
- Table 8. Tensile Properties of Corona-5 Alloy
- Table 9. Tensile Properties of Ti-6Al-4V Alloy

## LIST OF FIGURES

- Figure 1. WOL fatigue crack growth test specimen geometry.
- Figure 2. WOL specimen with clip gauge attached.
- Figure 3. Schematic illustration of load versus crack opening displacement.
- Figure 4. Fatigue crack growth rate of Corona-5 water quenched from 870°C.
- Figure 5. Fatigue crack growth rate of Corona-5 water quenched from 900°C.
- Figure 6. Fatigue crack growth rate of Corona-5 water quenched from 915°C.
- Figure 7. Fatigue crack growth rate of Corona-5 water quenched from 965°C.
- Figure 8. Fatigue crack growth rate of mill annealed Corona-5.
- Figure 9. Fatigue crack growth rate of  $\alpha+\beta$  annealed Ti-6Al-4V.
- Figure 10. Fatigue crack growth rate of Ti-6Al-4V alloy.
- Figure 11. Fatigue crack growth rates of Corona-5 alloys.

Table 1. Fatigue Crack Propagation Data of Corona-5 Quenched from 870°C.

#	Cycle N/100	Crack Length a (10 <sup>-2</sup> m)	Stress Intensity Range ΔK (MPa √m)	Crack Growth Rate da/dn (10 <sup>-8</sup> m/cycle)
1	0	2.8123	13.3547	4.0870
2	372	2.9579	14.0655	4.3861
3	649	3.0742	14.6859	5.0638
4	902	3.2112	15.4881	5.8723
5	1093	3.3197	16.1878	7.2141
6	1265	3.4409	17.0502	9.2002
7	1395	3.5636	18.0237	11.5508
8	1532	3.7285	19.5226	15.1280
9	1639	3.8983	21.3482	20.1712
10	1694	4.0150	22.8076	25.7649
11	1748	4.1563	24.8496	34.7977
12	1788	4.2930	27.1749	47.4703
13	1818	4.4426	30.2089	68.5479

Table 2. Fatigue Crack Propagation Data of Corona-5  
Quenched from 900°C.

#	Cycle N/100	Crack Length a (10 <sup>-2</sup> m)	Stress Intensity Range ΔK (MPa √m)	Crack Growth Rate da/dn (10 <sup>-8</sup> m/cycle)
1	0	2.2000	10.8719	2.2293
2	457	2.2936	11.2571	2.6623
3	497	2.3037	11.2948	2.7914
4	1212	2.5194	12.1309	3.8513
5	1496	2.6219	12.5566	4.7923
6	1752	2.7539	13.1391	5.7304
7	1972	2.8873	13.7759	6.6369
8	2194	3.0433	14.5959	7.9169
9	2311	3.1386	15.1441	9.3441
10	2419	3.2387	15.7664	11.0240
11	2513	3.3384	16.4396	13.1736
12	2592	3.4441	17.2194	15.5067
13	2702	3.6322	18.8100	19.7523
14	2774	3.7806	20.2901	24.1910
15	2827	3.9131	21.8185	30.4629
16	2872	4.0558	23.7331	38.4152
17	2905	4.1812	25.6953	48.6643
18	2929	4.3076	27.9955	65.0908
19	2938	4.3649	29.1648	82.0643
20	2949	4.4558	31.2068	107.6477

Table 3. Fatigue Crack Propagation Data of Corona-5  
Quenched from 915°C.

#	Cycle N/100	Crack Length a (10 <sup>-2</sup> m)	Stress Intensity Range $\Delta K$ (MPa $\sqrt{m}$ )	Crack Growth Rate da/dn (10 <sup>-8</sup> m/cycle)
1	0	2.4871	11.0162	2.6317
2	82	2.5112	11.1046	3.2867
3	226	2.5579	11.2789	3.2356
4	657	2.7124	11.8838	4.2801
5	737	2.7444	12.0156	4.5590
6	1206	3.0002	13.1668	6.8127
7	1331	3.0741	13.5382	8.5761
8	1451	3.1732	14.0703	8.9953
9	1557	3.2936	14.7743	9.7959
10	1651	3.3859	15.3648	10.0671
11	1744	3.4855	16.0581	10.4684
12	1819	3.5551	16.5812	10.7273
13	1885	3.6265	17.1556	11.0865
14	1947	3.7027	17.8136	11.8860
15	2009	3.7731	18.4683	12.7312
16	2068	3.8424	19.1605	15.0654
17	2124	3.9257	20.0620	18.5048
18	2172	4.0172	21.1525	22.4212
19	2220	4.1343	22.7211	27.3047
20	2255	4.2363	24.2743	31.7169
21	2287	4.3432	26.1235	37.3240
22	2310	4.4271	27.7593	45.4753
23	2329	4.5110	29.5870	59.7606

Table 4. Fatigue Crack Propagation Data of Corona-5  
Quenched from 965°C.

#	Cycle N/100	Crack Length a (10 <sup>-2</sup> m)	Stress Intensity Range $\Delta K$ (MPa $\sqrt{m}$ )	Crack Growth Rate da/dn (10 <sup>-8</sup> m/cycle)
1	0	2.2877	11.3191	1.3831
2	6	2.2916	11.3336	1.1984
3	573	2.3724	11.6397	1.6051
4	1016	2.4400	11.9025	1.7565
5	2282	2.6818	12.9110	3.0350
6	2815	2.8455	13.6717	4.0105
7	3100	2.9645	14.2759	4.6461
8	3744	3.3031	16.3149	6.3063
9	3861	3.3745	16.8215	7.0635
10	4048	3.5168	17.9334	8.2595
11	4290	3.7183	19.7877	11.8748
12	4367	3.8148	20.8177	14.8265
13	4429	3.9053	21.8848	19.0448
14	4480	4.0045	23.1840	22.9519
15	4516	4.0874	24.3801	26.0192
16	4547	4.1718	25.7271	28.4759
17	4573	4.2518	27.1353	29.6169
18	4596	4.3222	28.4969	28.8262
19	4611	4.3677	29.4413	28.1889
20	4629	4.4164	30.5173	28.3555
21	4644	4.4573	31.4768	29.6108
22	4658	4.4982	32.4869	30.1708
23	4669	4.5316	33.3583	30.3375
24	4679	4.5648	34.2610	32.0390

Table 4. Fatigue Crack Propagation Data of Corona-5  
Quenched from 965°C. (continued)

#	Cycle N/100	Crack Length a (10 <sup>-2</sup> m)	Stress Intensity Range $\Delta K$ (MPa $\sqrt{m}$ )	Crack Growth Rate da/dn (10 <sup>-8</sup> m/cycle)
25	4690	4.5993	35.2462	34.0923
26	4700	4.6320	36.2277	34.9478
27	4708	4.6604	37.1168	36.0278
28	4716	4.6913	38.1300	39.4421
29	4724	4.7246	39.2716	40.8706
30	4732	4.7556	40.3879	44.7641
31	4738	4.7821	41.6078	45.7471

Table 5. Fatigue Crack Propagation Data of  
Mill Annealed Corona-5

#	Cycle N/100	Crack Length a ( $10^{-2}$ m)	Stress Intensity Range $\Delta K$ (MPa $\sqrt{\text{m}}$ )	Crack Growth Rate da/dn ( $10^{-8}$ m/cycle)
1	0	1.4929	8.4667	1.2339
2	985	1.6203	8.8988	1.5586
3	1702	1.7415	9.3080	1.7286
4	2081	1.8096	9.5382	1.8197
5	3085	1.9921	10.1601	1.8883
6	3814	2.1344	10.6559	2.1512
7	4118	2.2015	10.8947	2.7927
8	4410	2.3009	11.2567	3.4970
9	4705	2.3960	11.6431	3.2759
10	5004	2.5017	12.0265	3.5845
11	5223	2.5788	12.3394	4.7463
12	5387	2.6676	12.7147	5.4064
13	5498	2.7281	12.9806	5.9710
14	5680	2.8385	13.4904	6.6121
15	5908	3.0195	14.4079	8.4803
16	6063	3.1578	15.1933	10.3381
17	6140	3.2394	15.6975	10.8924
18	6250	3.3770	16.6284	13.0211
19	6340	3.4975	17.5430	15.0990
20	6400	3.5929	18.5592	17.3476
21	6461	3.7056	19.3800	20.4225
22	6542	3.8800	21.2479	26.6423
23	6606	4.0649	23.7466	34.9793
24	6650	4.2406	26.4488	44.5637

Table 5. Fatigue Crack Propagation Data of  
Mill Annealed Corona-5 (continued)

#	Cycle N/100	Crack Length a (10 <sup>-2</sup> m)	Stress Intensity Range ΔK (MPa √m)	Crack Growth Rate da/dn (10 <sup>-8</sup> m/cycle)
25	6689	4.4296	30.2145	63.3039
26	6717	4.6300	35.3743	88.1941
27	6733	4.7850	40.5040	113.6456
28	6742	4.8983	44.8801	148.0832
29	6748	4.9880	49.4102	172.7466

Table 6. Fatigue Crack Propagation Data of  $\alpha+\beta$  Annealed Ti-6Al-4V

#	Cycle N/100	Crack Length a ( $10^{-2}$ m)	Stress Intensity Range $\Delta K$ (MPa $\sqrt{m}$ )	Crack Growth Rate da/dn ( $10^{-8}$ m/cycle)
1	0	1.9075	12.5004	1.2319
2	400	1.9583	12.7270	1.5976
3	750	2.0142	13.0152	2.0193
4	1130	2.0904	13.3782	2.2656
5	1520	2.1793	13.8435	3.5356
6	1870	2.2987	14.3737	4.1021
7	2140	2.4079	14.9952	6.9189
8	2350	2.5527	15.7102	8.8900
9	2500	2.6873	16.4142	10.2438
10	2620	2.8092	17.1413	13.6321
11	2710	2.9311	18.0312	17.1018
12	2800	3.1788	18.9200	17.7342
13	2855	3.1826	19.7549	21.4757
14	2910	3.2994	20.8758	26.2305
15	2965	3.4467	22.1705	31.3690
16	3005	3.5712	23.5950	38.9712
17	3040	3.7084	25.1086	43.7896
18	3065	3.8176	26.9291	60.0456
19	3090	3.9674	29.0664	76.2000
20	3105	4.0817	30.9837	93.4720
30	3115	4.1757	33.7601	153.0934

Table 7. Fatigue Crack Propagation Data of Ti-6Al-4V  
Quenched from 900°C.

#	Cycle N/100	Crack Length a (10 <sup>-2</sup> m)	Stress Intensity Range ΔK (MPa √m)	Crack Growth Rate da/dn (10 <sup>-8</sup> m/cycle)
1	0	1.8770	13.4915	1.1531
2	400	1.9227	13.7071	1.5189
3	700	1.9685	13.9227	1.7830
4	1000	2.0218	14.1746	2.5984
5	1500	2.1513	14.8049	3.5585
6	1800	2.2580	15.3362	4.9530
7	2000	2.3571	15.8444	4.9530
8	2200	2.4561	16.3713	6.5532
9	2400	2.5882	17.1094	7.6200
10	2550	2.7025	17.7870	10.1219
11	2700	2.8549	18.7627	10.4190
12	2800	2.9591	19.4854	16.4465
13	2880	3.0911	20.4809	20.1930
14	2920	3.1724	21.1442	23.3680
15	2945	3.2308	21.6480	28.7858

Table 8: Tensile Properties of Corona-5 Specimens Water Quenched from the Designated Temperature in °C.

Specimen	Yield Stress	Ultimate Tensile Stress	Young's Modulus
Heat Treatment	$10^8$ N/m <sup>2</sup> (KSI)	$10^8$ N/m <sup>2</sup> (KSI)	$10^{10}$ N/m <sup>2</sup> ( $10^6$ PSI)
Mill Anneal	9.43 (137)	10.1 (147)	11.5 (16.6)
870°C (1600°F)	4.6 (66.7)	10.4 (150.7)	8.20 (11.9)
900°C (1650°F)	4.20 (61.1)	10.4 (151)	7.70 (11.2)
915°C (1680°F)	3.37 (48.9)	11.00 (160)	8.55 (12.4)
965°C (1770°F)	7.93 (115)	10.8 (157)	9.94 (14.4)

Table 9: Tensile Properties of Ti-6Al-4V Specimens

Specimen	Yield Stress	Ultimate Tensile Stress	Young's Modulus
Heat Treatment	$10^8$ N/m <sup>2</sup>	$10^8$ N/m <sup>2</sup> (KSI)	$10^{10}$ N/m <sup>2</sup> (KSI) ( $10^6$ PSI)
Annealed	8.99 (130)	9.90 (144)	10.3 (15.0)
900°C+ Water Quench	9.98 (145)	11.58 (168)	11.6 (16.8)

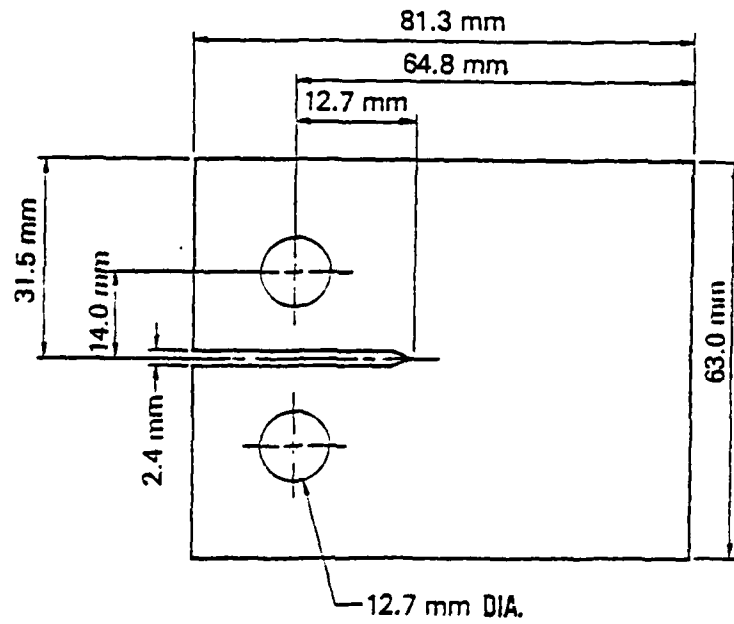


Figure 1. WOL fatigue crack growth test specimen geometry.

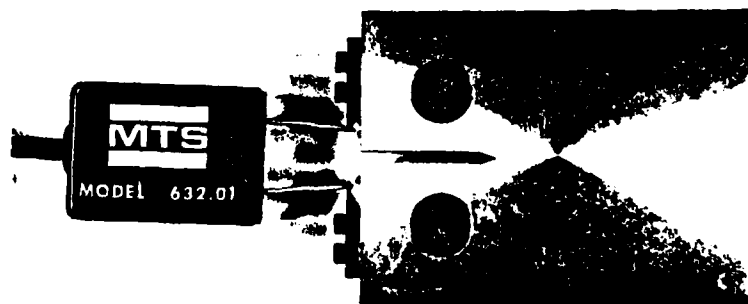


Figure 2. WOL specimen with clip gage attached.

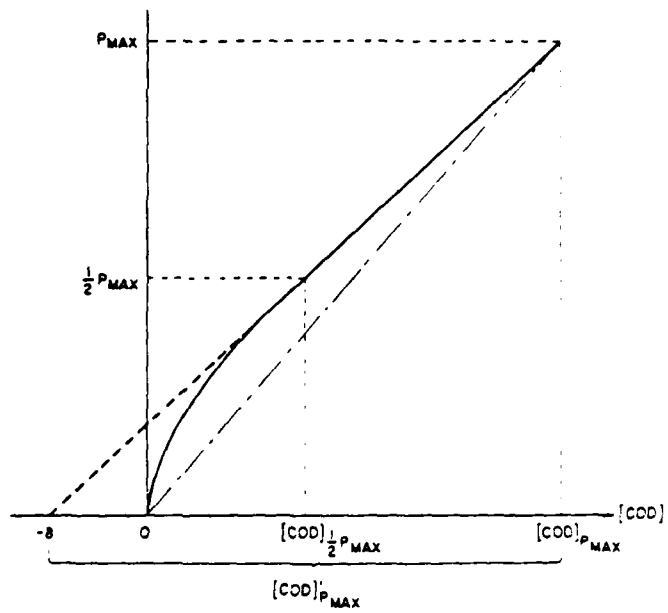


Figure 3. Schematic illustration of load versus crack opening displacement.

Figure 4. Fatigue Crack Growth Rate of CORONA-5 Water Quenched from 870°C. Specimen Thickness was 1.016 cm and  $P_{max}$  was 0.454 Newtons.

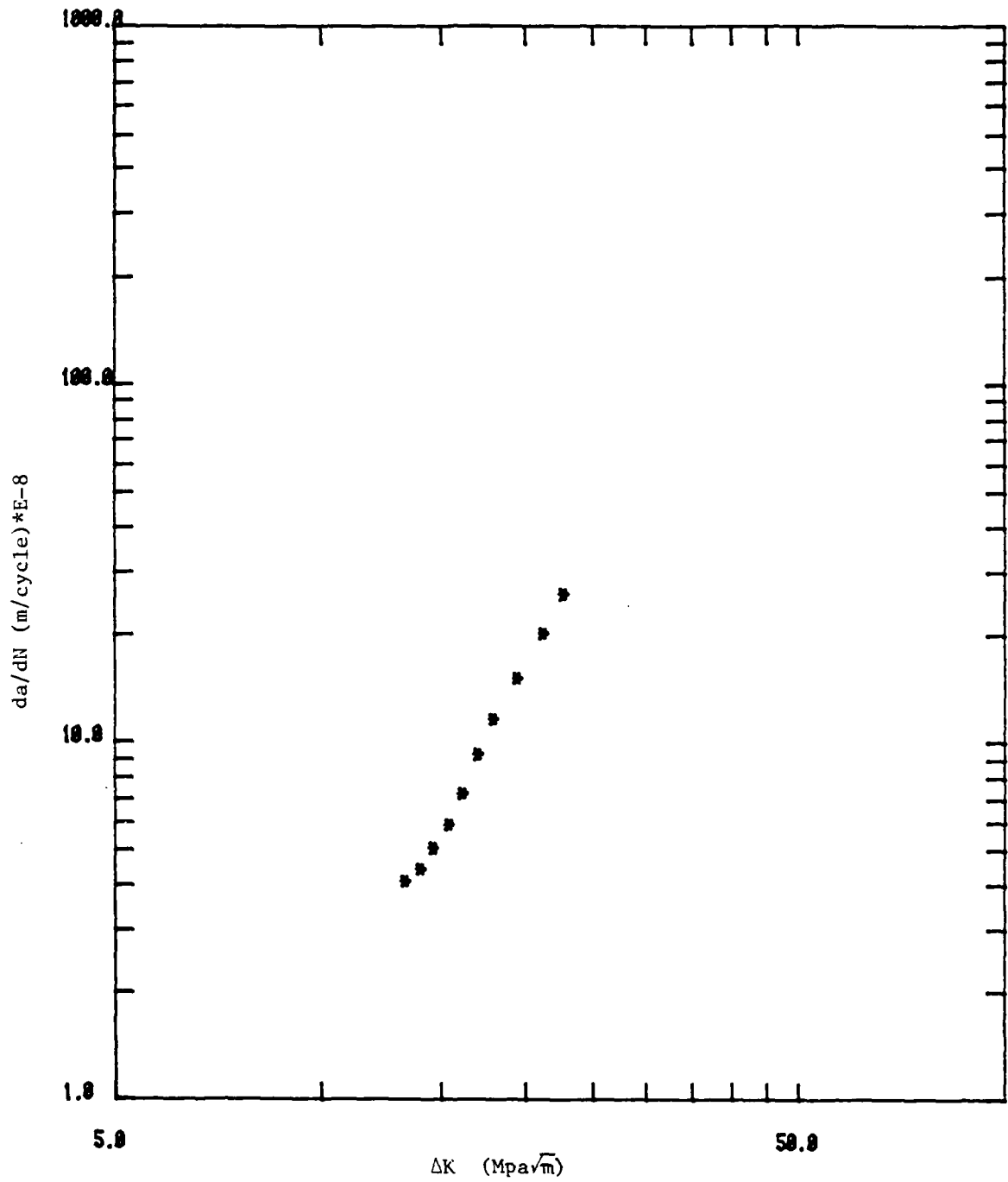


Figure 5. Fatigue Crack Growth Rate of CORONA-5 Water Quenched from 900°C. Specimen Thickness was 1.016 cm and  $P_{max}$  was 0.454 Newtons.

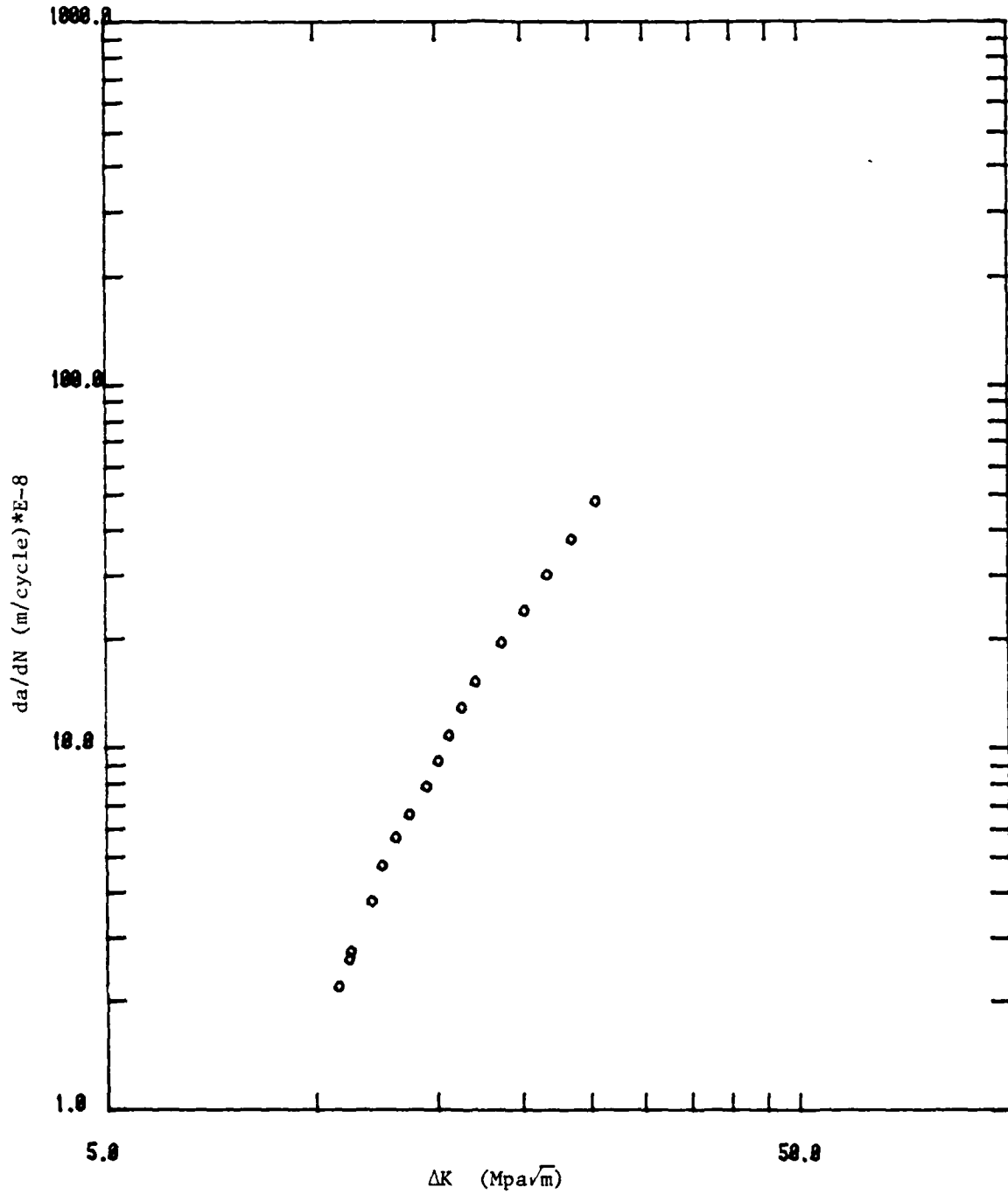


Figure 6. Fatigue Crack Growth Rate of CORONA-5 Water Quenched from 915°C.  
Specimen Thickness was 1.016 cm and  $P_{max}$  was 0.454 Newtons.

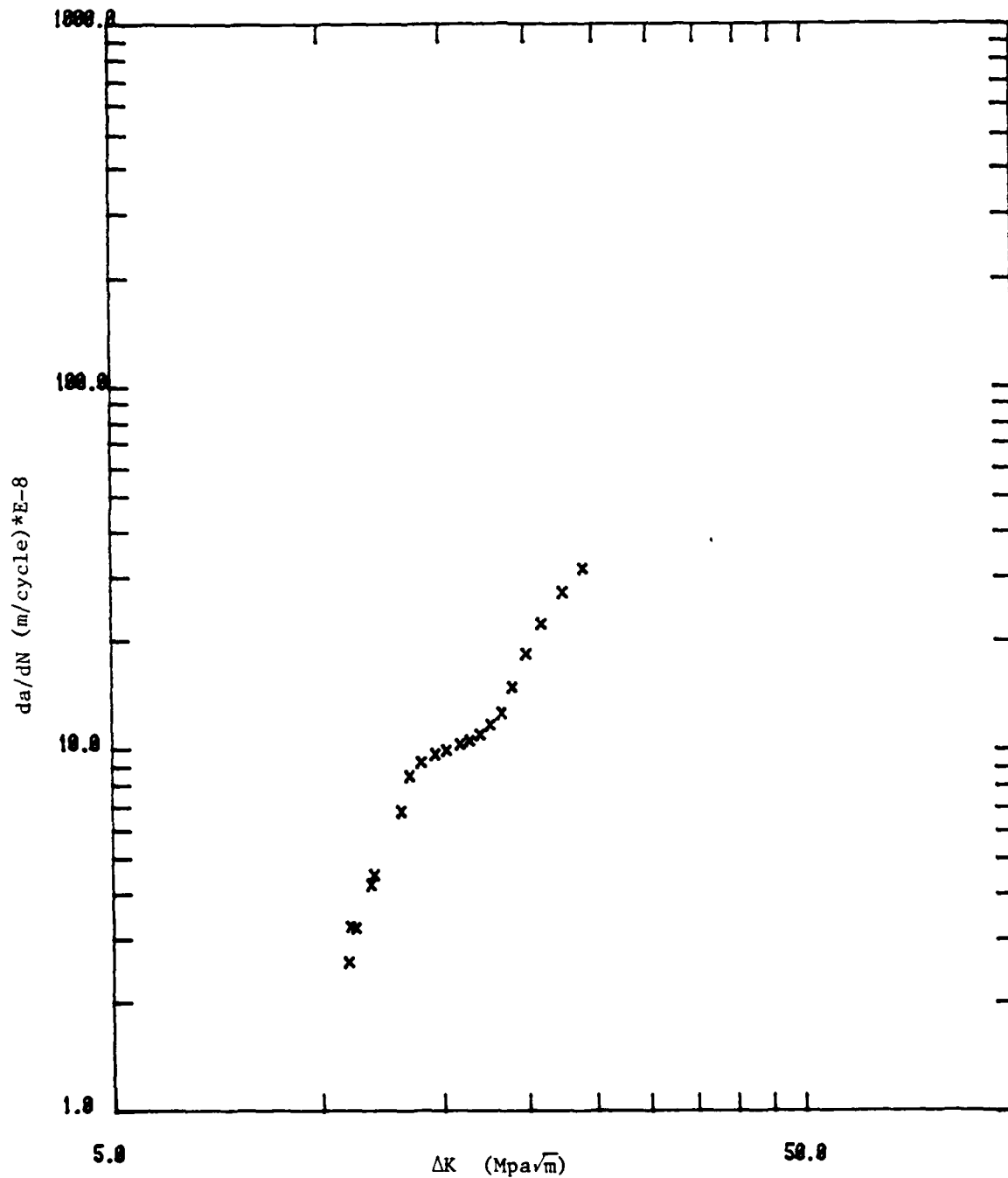


Figure 7. Fatigue Crack Growth Rate CORONA-5 water quenched from 965°C.  
Specimen Thickness was 1.016 cm and  $P_{max}$  was 0.454 Newtons.

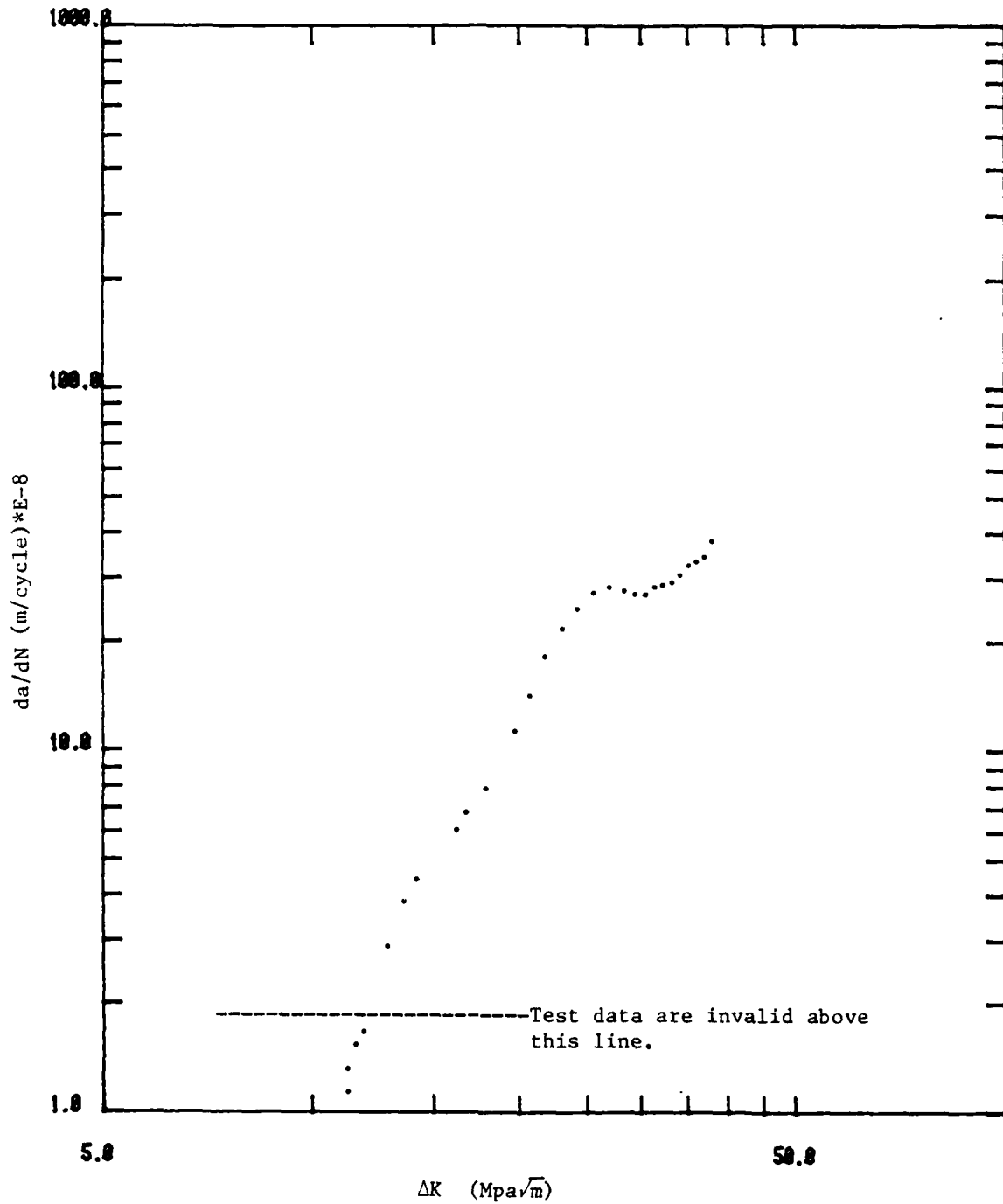


Figure 8. Fatigue Crack Growth Rate of mill annealed CORONA-5.  
Specimen Thickness was 1.016 cm and  $P_{max}$  0.454 Newtons.

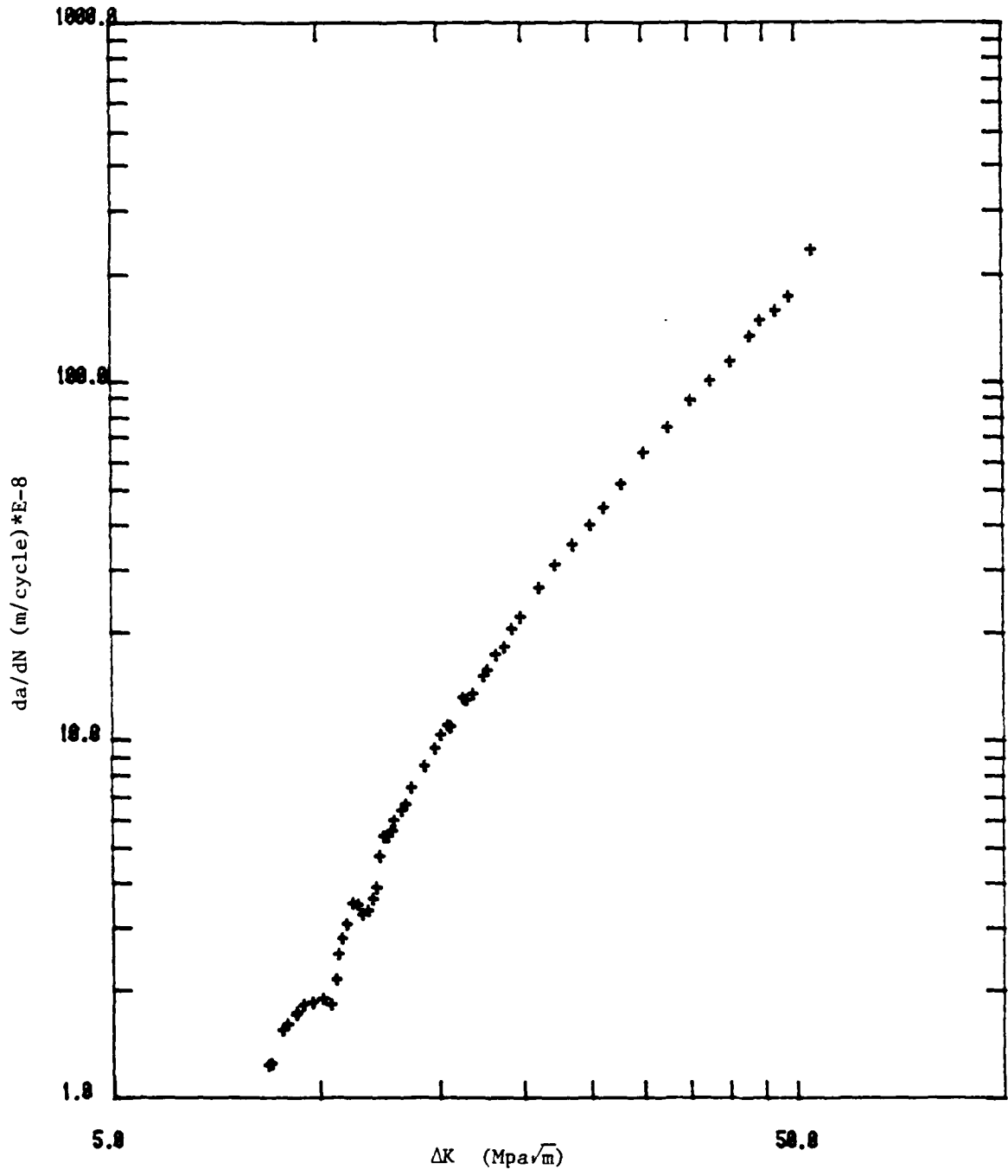


Figure 9. Fatigue Crack Growth Rate of  $\alpha+\beta$  Annealed Ti-6Al-4V.  
Specimen was 2.54 cm and  $P_{max}$  was 1.362 Newtons.

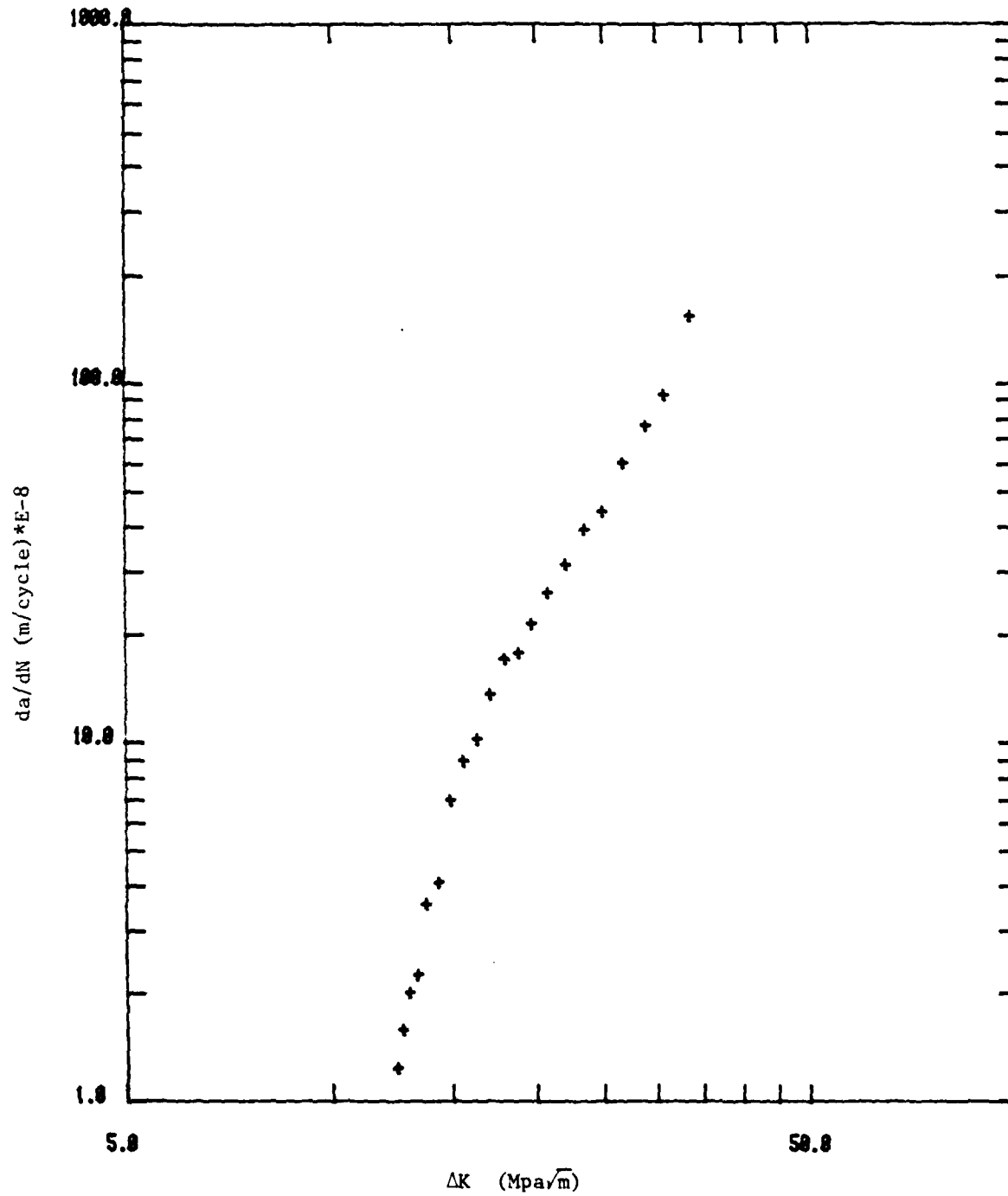


Figure 10. Fatigue Crack Growth Rate of Ti-6Al-4V Alloy  
 The Annealed Specimen Thickness was 2.54 cm and the as  
 Quenched Specimen Thickness was 1.27 cm.  
 $P_{max}$  of Annealed Specimen was 1.362 Newtons and  $P_{max}$   
 for as Quenched Specimen was 0.908 Newtons.

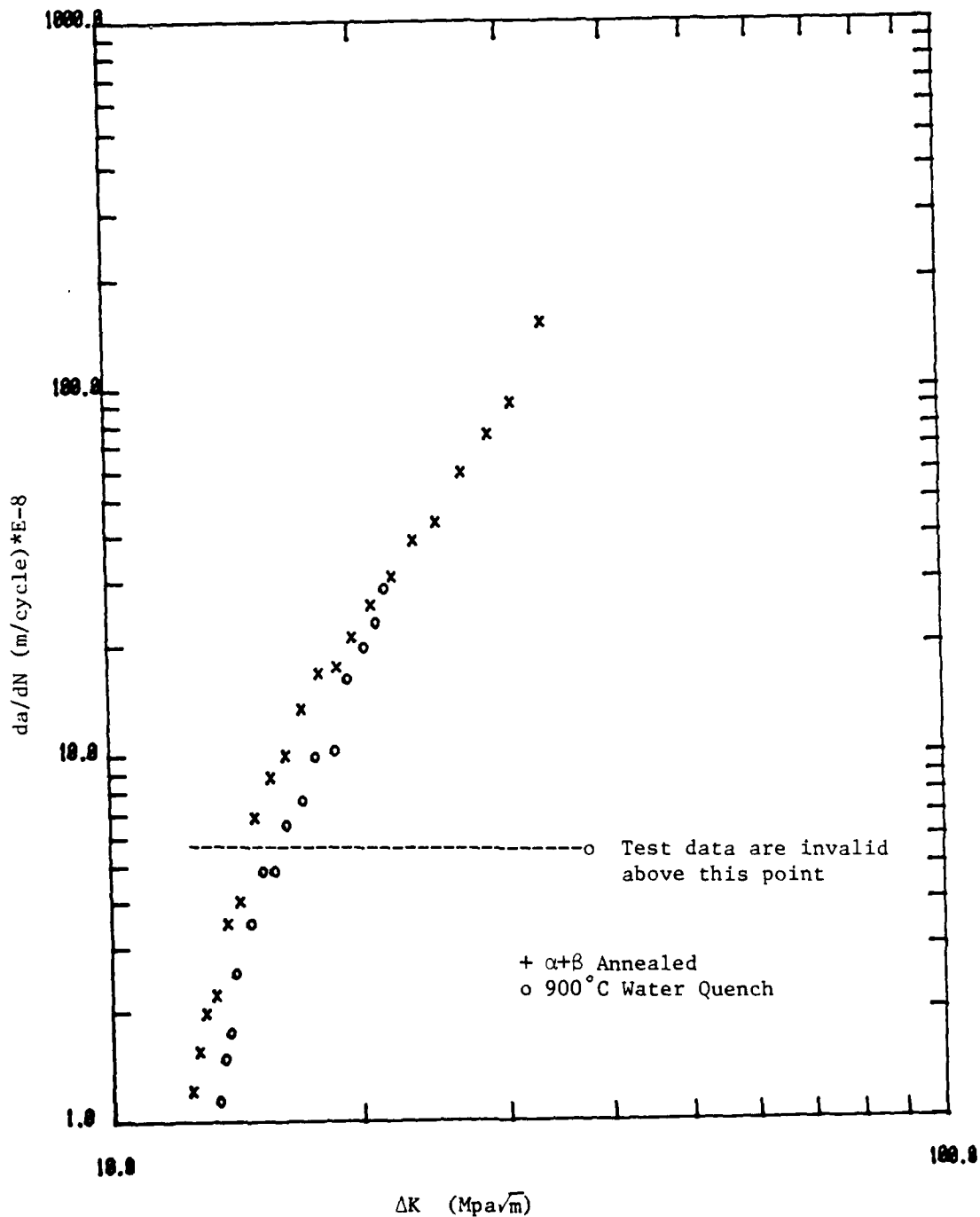
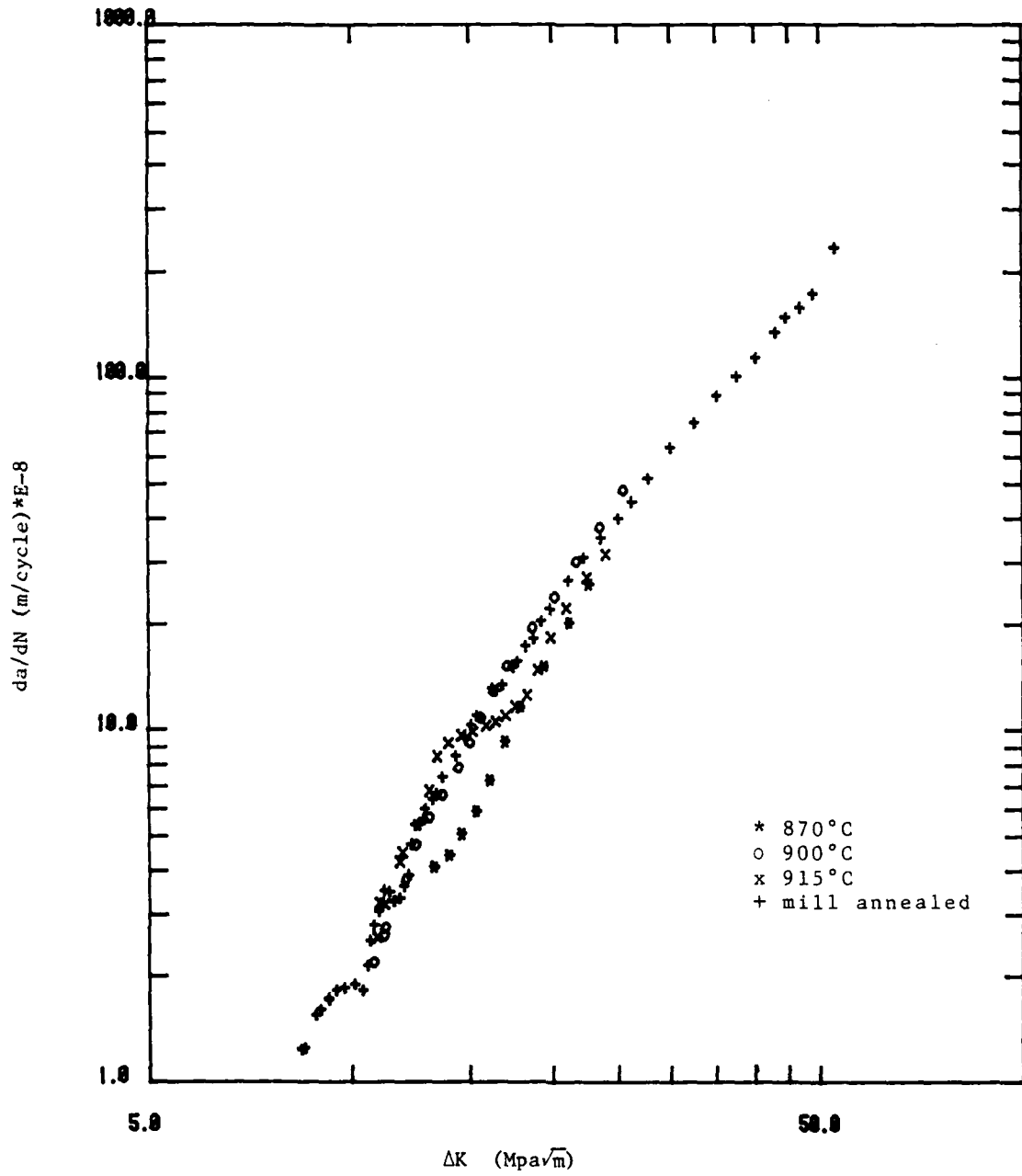


Figure 11. Fatigue Crack Growth Rates of CORONA-5 Alloys.  
Specimen Thickness was 10.16 cm and  $P_{max}$  was 0.454 Newtons.



## REPORT DOCUMENTATION PAGE

1a. REPORT SECURITY CLASSIFICATION Unclassified		1b. RESTRICTIVE MARKINGS None	
2a. SECURITY CLASSIFICATION AUTHORITY Not Applicable		3. DISTRIBUTION/AVAILABILITY OF REPORT Distribution for Public Release <b>APPROVED FOR PUBLIC RELEASE: DISTRIBUTION UNLIMITED</b>	
2b. DECLASSIFICATION/DOWNGRADING SCHEDULE Not Applicable			
4. PERFORMING ORGANIZATION REPORT NUMBER(S) GWU-CMEE-TR-84-1		5. MONITORING ORGANIZATION REPORT NUMBER(S)	
6a. NAME OF PERFORMING ORGANIZATION The George Washington University	6b. OFFICE SYMBOL (If applicable)	7a. NAME OF MONITORING ORGANIZATION	
6c. ADDRESS (City, State and ZIP Code) School of Engineering and Applied Science Washington, D.C. 20052		7b. ADDRESS (City, State and ZIP Code)	
8a. NAME OF FUNDING/SPONSORING ORGANIZATION Naval Air Systems Command	8b. OFFICE SYMBOL (If applicable)	9. PROCUREMENT INSTRUMENT IDENTIFICATION NUMBER N00019-82-C-0170	
8c. ADDRESS (City, State and ZIP Code) Washington, D.C. 20361		10. SOURCE OF FUNDING NOS.	
		PROGRAM ELEMENT NO.	PROJECT NO.
		TASK NO.	WORK UNIT NO.
11. TITLE (Include Security Classification) Unclassified Fatigue Crack Propagation in Metastable Ti Alloys			
12. PERSONAL AUTHOR(S) S. H. Yang, A. Raith, C. M. Gilmore, and M. A. Imam			
13a. TYPE OF REPORT Technical	13b. TIME COVERED FROM 3/31/82 TO 3/31/83	14. DATE OF REPORT (Yr., Mo., Day)	15. PAGE COUNT
16. SUPPLEMENTARY NOTATION			
17. COSATI CODES		18. SUBJECT TERMS (Continue on reverse if necessary and identify by block number)	
FIELD	GROUP	SUB. GR.	
19. ABSTRACT (Continue on reverse if necessary and identify by block number)			
<p>The fatigue crack growth rate tests of water quenched Corona-5 (Ti-4.5Al-1.5Cr-5Mo) and Ti-6Al-4V alloy were conducted in air at room temperature. The effect of the presence of the metastable retained <math>\beta</math> phase on the fatigue crack growth rate was examined in this research. The specimens were heat treated and water quenched to have unstable <math>\beta</math> phase that could be transformed to martensite during the fatigue crack growth testing. As quenched specimens were compared with specimens in the mill annealed condition. The fatigue crack growth rates of all the specimens were in the same order of magnitude regardless of the heat treatment. From this research it was shown that, in Corona-5 and Ti-6Al-4V alloy, fatigue crack growth rates were not affected by the strain induced martensitic transformation. The yield strength of the specimens in this research varied from 337 Mpa (48.9 ksi) to 947 Mpa (137 ksi). This also demonstrated that the fatigue crack growth rates of Corona-5 and Ti-6Al-4V alloys in these conditions were independent of the yield strength.</p>			
20. DISTRIBUTION/AVAILABILITY OF ABSTRACT UNCLASSIFIED/UNLIMITED <input checked="" type="checkbox"/> SAME AS RPT. <input type="checkbox"/> DTIC USERS <input type="checkbox"/>		21. ABSTRACT SECURITY CLASSIFICATION	
22a. NAME OF RESPONSIBLE INDIVIDUAL Charles M. Gilmore		22b. TELEPHONE NUMBER (Include Area Code) (202) 676-6903	22c. OFFICE SYMBOL

**THE GEORGE WASHINGTON UNIVERSITY**

**BENEATH THIS PLAQUE  
IS BURIED  
A VAULT FOR THE FUTURE  
IN THE YEAR 2056**

**THE STORY OF ENGINEERING IN THIS YEAR OF THE PLACING OF THE VAULT AND  
ENGINEERING HOPES FOR THE TOMORROWS AS WRITTEN IN THE RECORDS OF THE  
FOLLOWING GOVERNMENTAL AND PROFESSIONAL ENGINEERING ORGANIZATIONS AND  
THOSE OF THIS GEORGE WASHINGTON UNIVERSITY.**

**BOARD OF COMMISSIONERS DISTRICT OF COLUMBIA  
UNITED STATES ATOMIC ENERGY COMMISSION  
DEPARTMENT OF THE ARMY UNITED STATES OF AMERICA  
DEPARTMENT OF THE NAVY UNITED STATES OF AMERICA  
DEPARTMENT OF THE AIR FORCE UNITED STATES OF AMERICA  
NATIONAL ADVISORY COMMITTEE FOR AERONAUTICS  
NATIONAL BUREAU OF STANDARDS U.S. DEPARTMENT OF COMMERCE  
AMERICAN SOCIETY OF CIVIL ENGINEERS  
AMERICAN INSTITUTE OF ELECTRICAL ENGINEERS  
THE AMERICAN SOCIETY OF MECHANICAL ENGINEERS  
THE SOCIETY OF AMERICAN MILITARY ENGINEERS  
AMERICAN INSTITUTE OF MINING AND METALLURGICAL ENGINEERS  
DISTRICT OF COLUMBIA SOCIETY OF PROFESSIONAL ENGINEERS, INC.  
THE INSTITUTE OF RADIO ENGINEERS, INC.  
THE CHEMICAL ENGINEERS CLUB OF WASHINGTON  
WASHINGTON SOCIETY OF ENGINEERS  
PAULINER, KINGSBURY & STENHOUSE - ARCHITECTS  
CHARLES H. TOMPKINS COMPANY - BUILDERS  
SOCIETY OF WOMEN ENGINEERS  
NATIONAL ACADEMY OF SCIENCES NATIONAL RESEARCH COUNCIL**

**THE PURPOSE OF THIS VAULT IS INSPIRED BY AND IS DEDICATED TO  
CHARLES HOOK TOMPKINS, DOCTOR OF ENGINEERING  
BECAUSE OF HIS ENGINEERING CONTRIBUTIONS TO THIS UNIVERSITY, TO HIS  
COMMUNITY, TO HIS NATION AND TO OTHER NATIONS.**

**BY THE GEORGE WASHINGTON UNIVERSITY.**

**ROBERT A. FLEMING  
CHAIRMAN OF THE BOARD OF TRUSTEES**

**CLOYD H. MARVIN  
PRESIDENT**

**FOUNDED THE TWENTIETH  
1909**

To cope with the expanding technology, our society must be assured of a continuing supply of rigorously trained and educated engineers. The School of Engineering and Applied Science is completely committed to this objective.